Improvements on fast live cell imaging at the nanoscale

Technical Journal Club
21.02.2017.
Orsolya Török

Why superresolution?

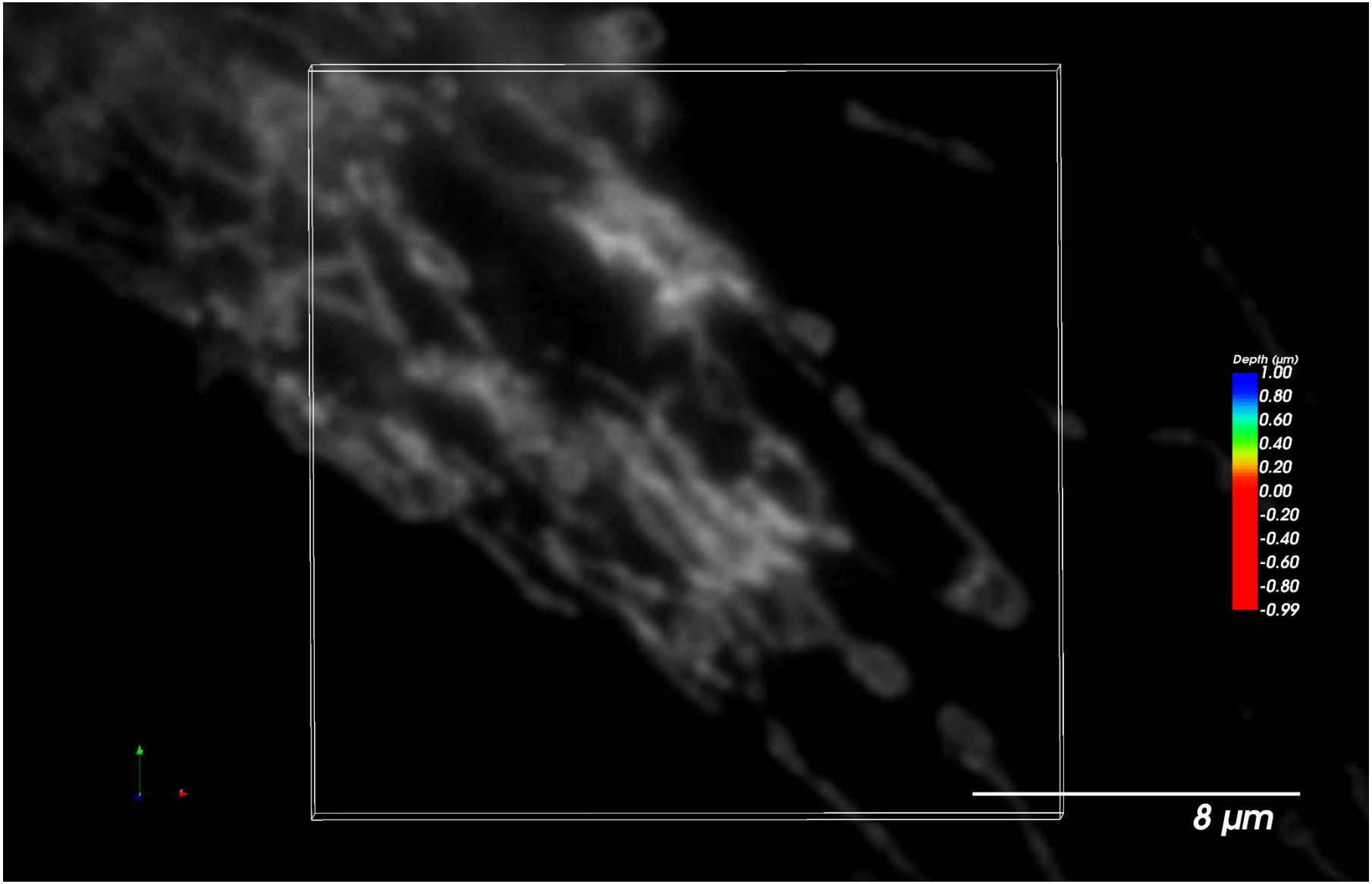

Mitochondria in HeLa cells

Image: Microscopy Winter School, UZH, 2017.

Why superresolution?

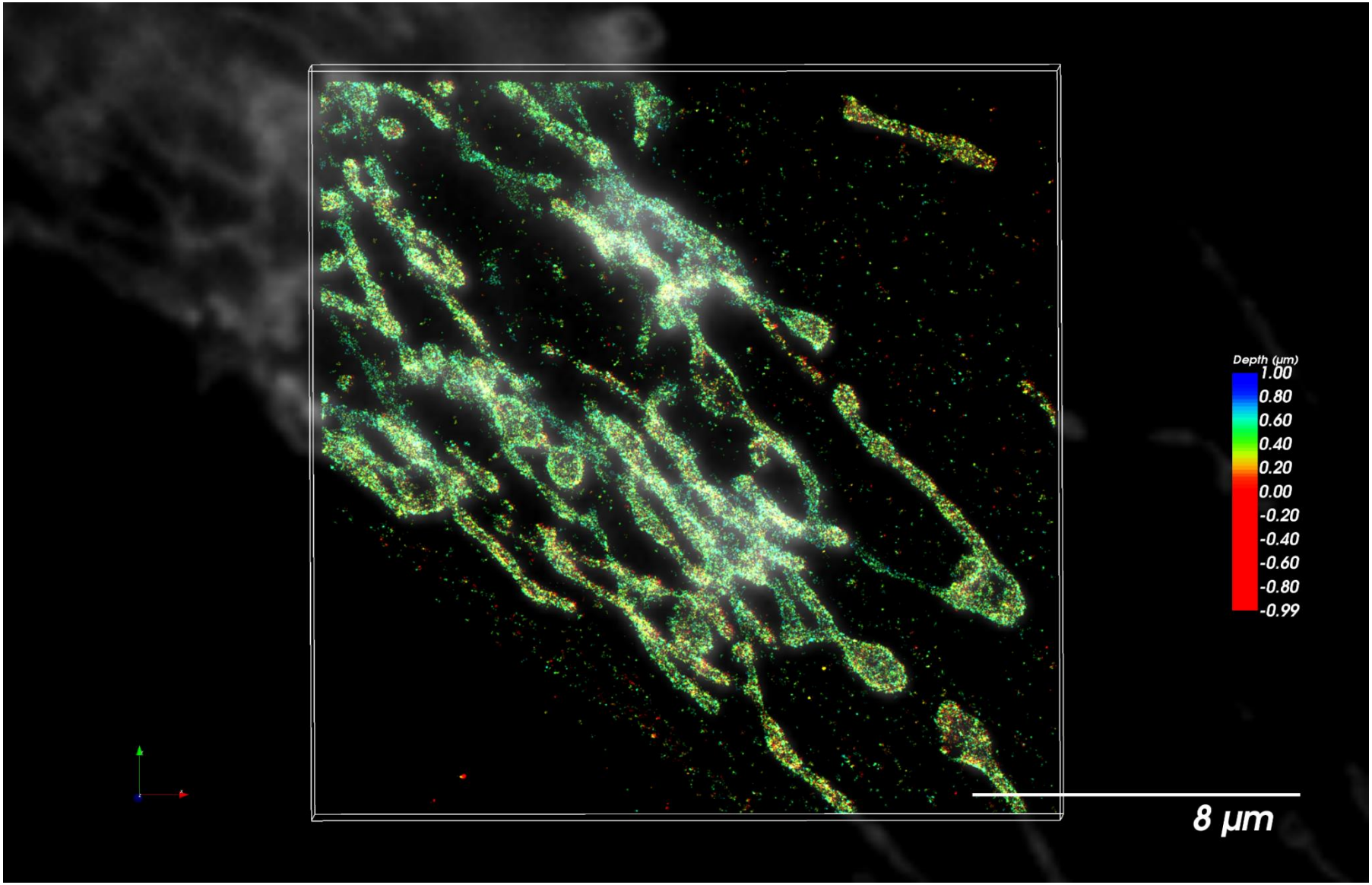

Mitochondria in HeLa cells

Image: Microscopy Winter School, UZH, 2017.

Resolution in light microscopy

The distance at which separate point sources become distinguishable.

The diffraction pattern of a point source of light

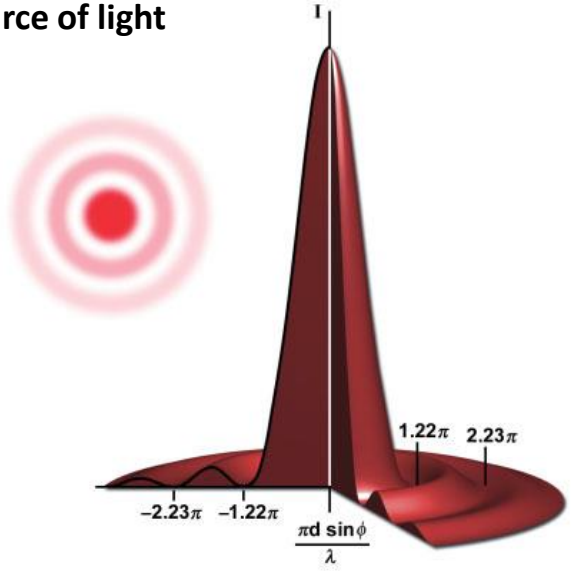

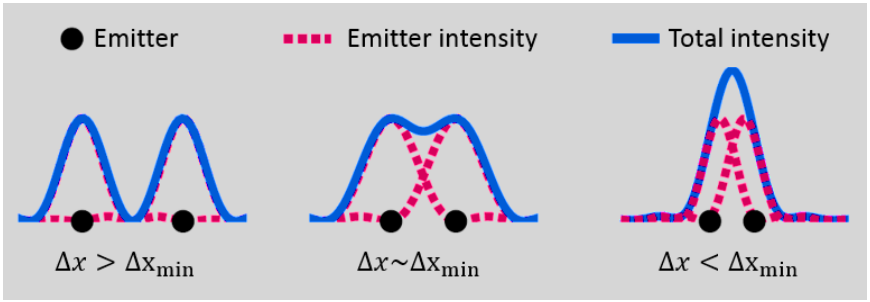

Object

Image

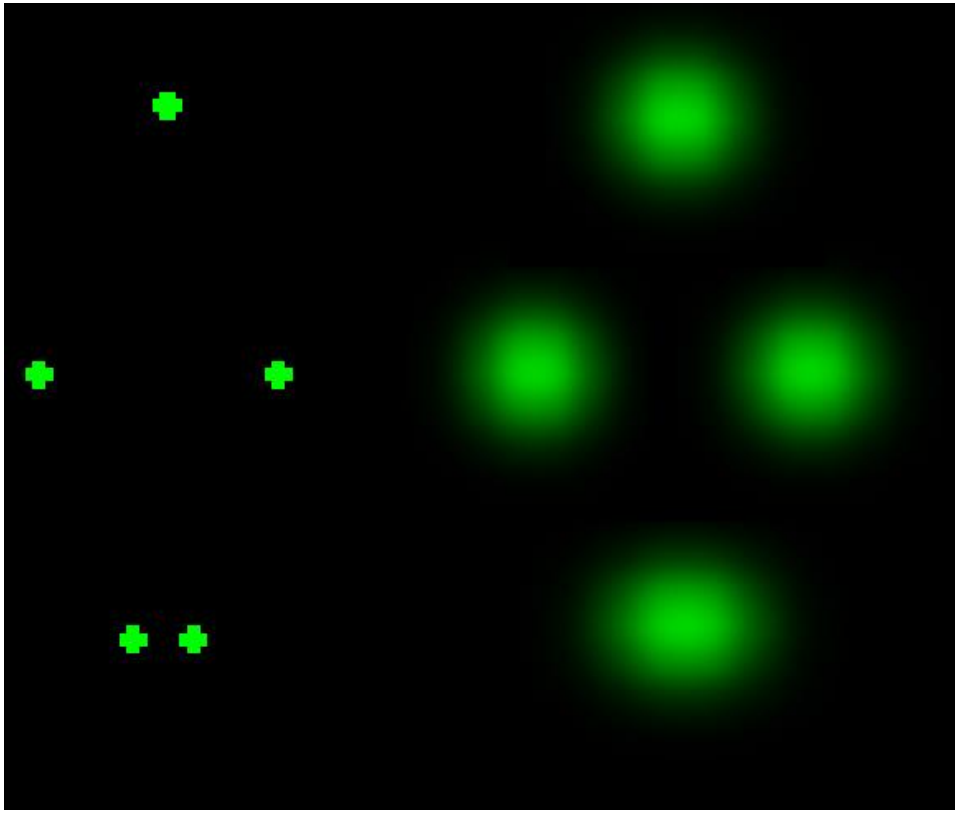

Douglas B. Murphy, Michael W. Davidson: Fundamentals of Light Microscopy and Electronic imaging

Resolution limit in light microscopy

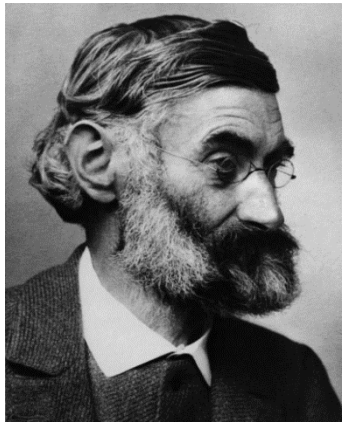

Ernst Abbé
(1840-1905)

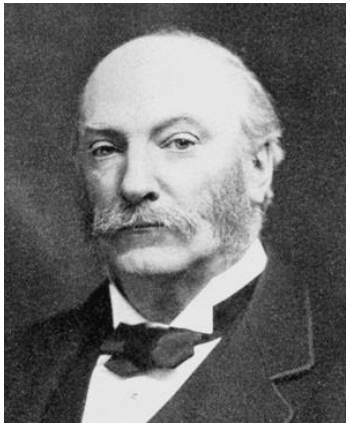

Lord Rayleigh
(1842-1919)

d = 1.22 λ/NA

By this criterion, two adjacent object points are defined as being resolved when the central diffraction spot (Airy disk) of one point coincides with the first diffraction minimum of the other point in the image plane.

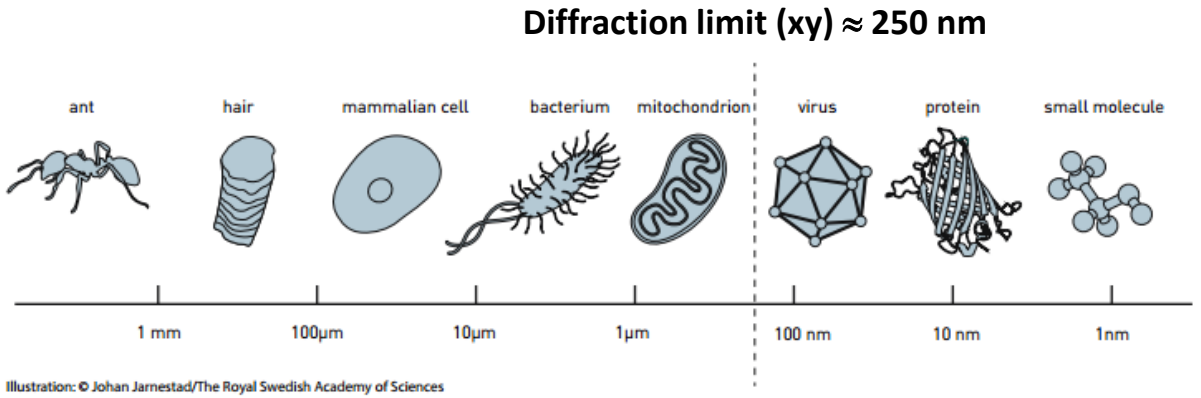

Douglas B. Murphy, Michael W. Davidson: Fundamentals of Light Microscopy and Electronic imaging

Confocal laser scanning microscope

The sample is illuminated with laser light focused to a diffraction limited spot.
The spot is scanned in a raster fashion over the sample to illuminate fluorescent dyes.
Emission of fluorescent light is detected through a pinhole located in a confocal plane relative to the plane of focus.

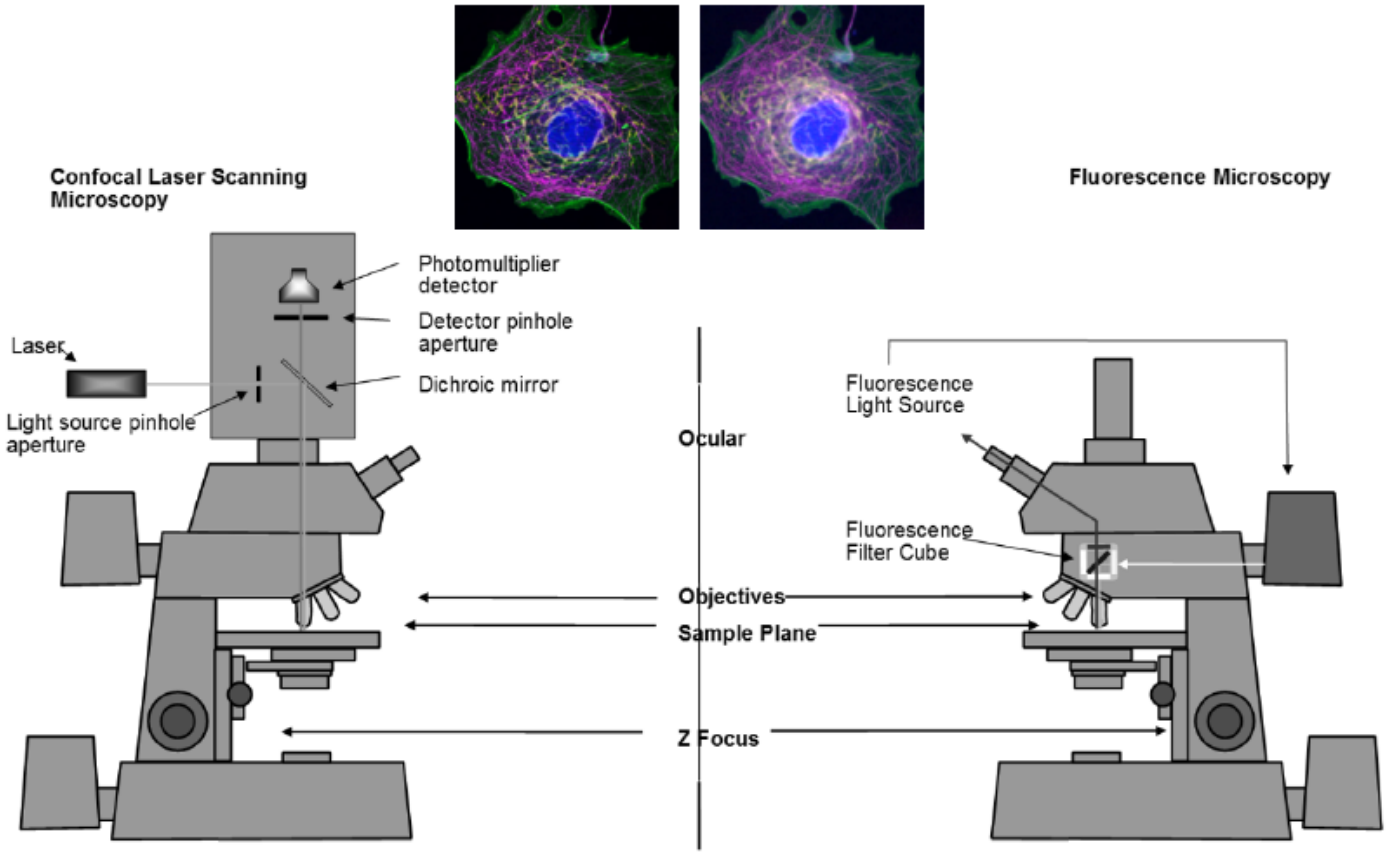

Douglas B. Murphy, Michael W. Davidson: Fundamentals of Light Microscopy and Electronic imaging

Super-resolved fluorescent microscopy

All microscopy techniques that achieve a resolution higher than that defined by Ernst Abbé (approx. 250nm in x,y axis and 600-750nm in z axis).

The Nobel Prize in Chemistry 2014

Eric Betzig

Stefan W. Hell

William E. Moerner

www.nobelprize.org

Types of superresololution microscopy

I. Localization microscopy methods (temporal separation of fluorophores):

- (F)PALM
- STROM
- dSTORM

10-30 nm
resolution in xy

II. Scanning methods (spatial separation of fluorophores):

- STED

50-90 nm
resolution in xy

III. Fourier methods:

- SIM

100-150 nm
resolution in xy

(STED) S. Hell, PNAS 105**,** 48, 18983, 2008.
(SIM) M. Gustafsson, Journal of Microscopy, 198, 2, 82-87, 2000.
((F)PALM) E. Betzig, Science, 313, 6142, 2006 and S. Hess, Biophysical Journal, 91,2006.
(STORM) M. Rust, Nature Methods, 3,10, 2006.
(dSTORM) M. Sauer, Angew. Chem.Int., 42,6172, 2008.

Localisation microscopy principles

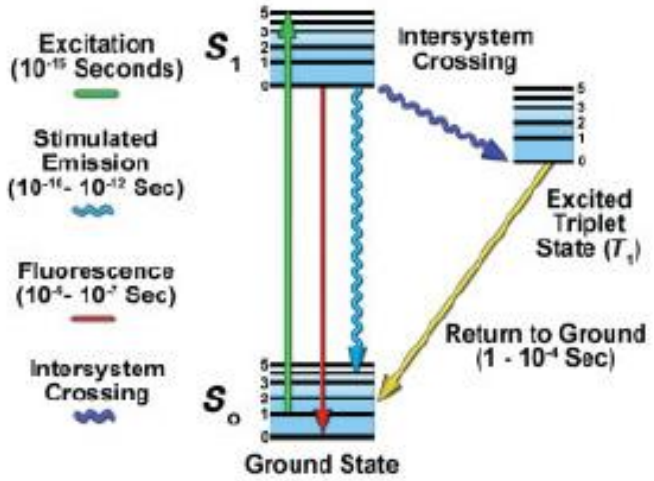

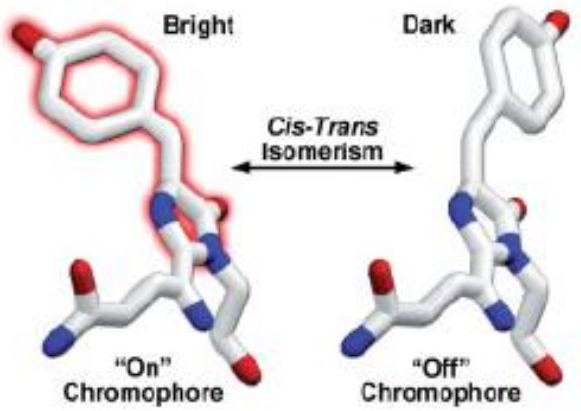

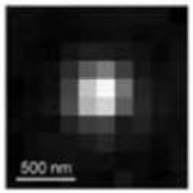

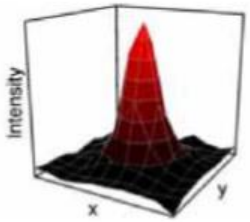

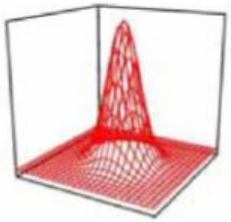

A single fluorescent object can be precisely localized by determining the center of its emission pattern by fitting a two-dimensional Gaussian profile to the individual point spread function (PSF).

Douglas B. Murphy, Michael W. Davidson: Fundamentals of Light Microscopy and Electronic imaging

STED principles

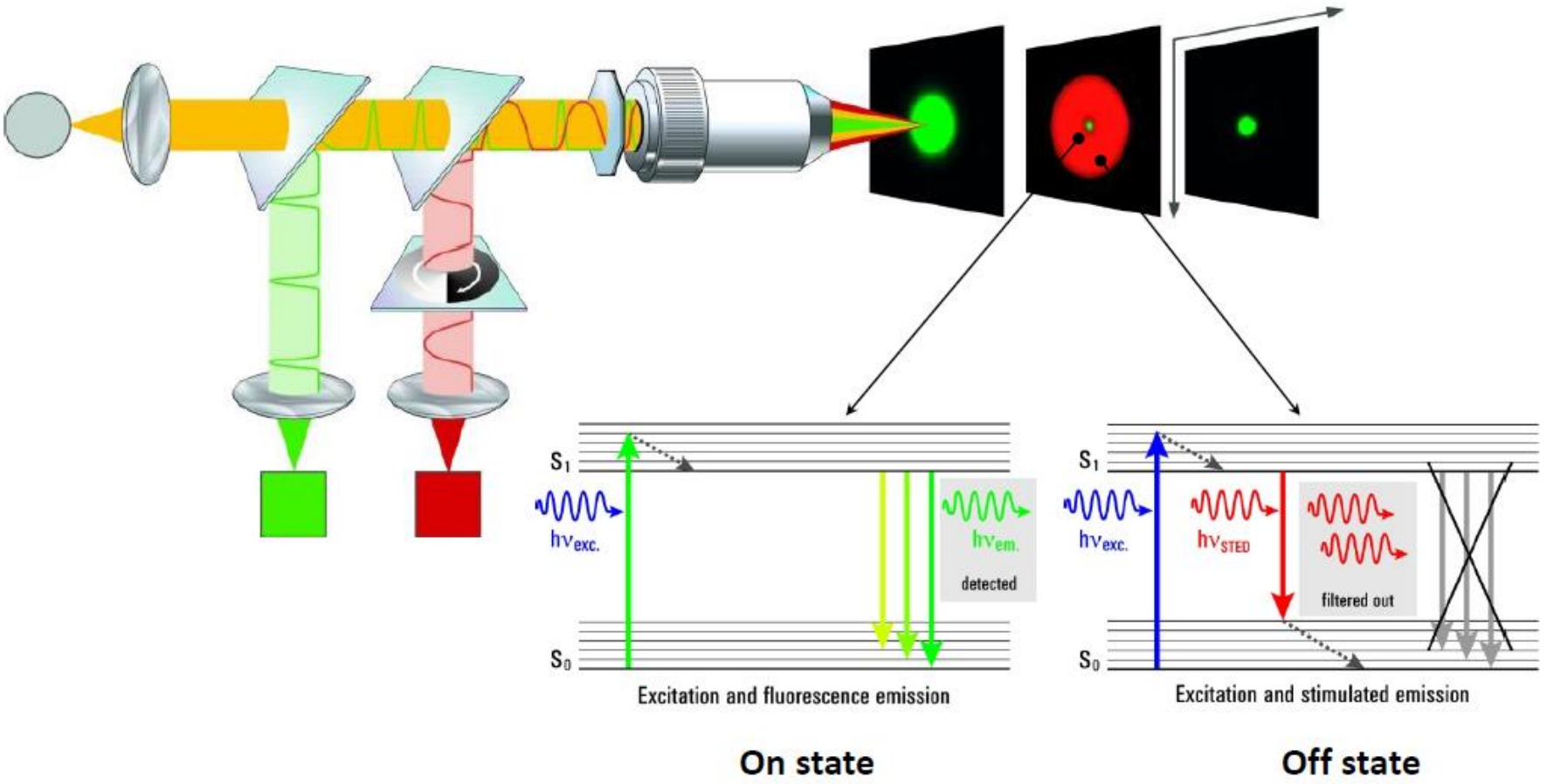

Leica, Microscopy Winter School 2017.

SIM principles

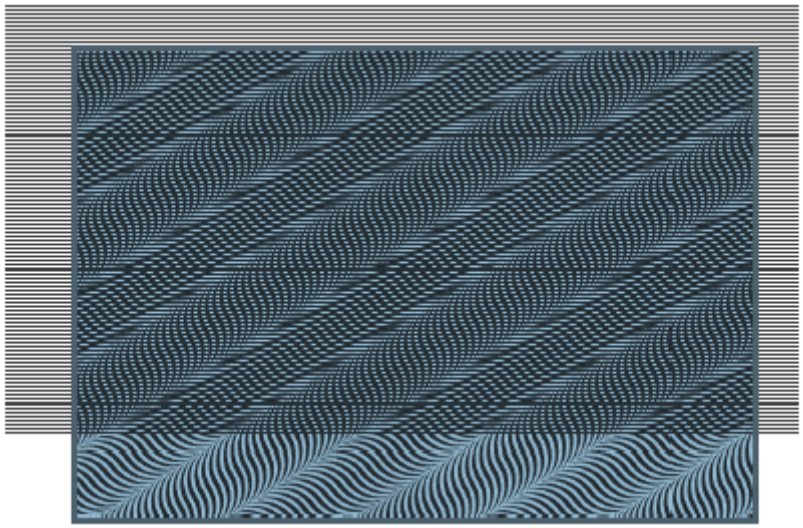

Two superimposed patterns (in this case the illumination pattern and the structures in the sample) interfere with each other and produce a third, characteristic pattern: the **Moiré fringes**.

Limitations in superresolution microscopy:

- special fluorophores and conditions (PALM, STORM)-structural cell biology
- requires specialized/expensive optical elements (SIM)-possible approach
- long acquisition time due to the collection of enough photon-counts- increased damage to cells (ROS, DNA impairment)
- high illumination intensities – increased damage

} Limited application in live cell imaging

Reversible cryo-arrest for imaging molecules in living cells at high spatial resolution

Martin E Masip[1,4], Jan Huebinger[1,4], Jens Christmann[1,2,4], Ola Sabet[1], Frank Wehner[1], Antonios Konitsiotis[1], Günther R Fuhr[3] & Philippe I H Bastiaens[1,2]

Rationale

- Molecular patterns in living cells can be highly dynamic – interferes with long acquisition times.
- Irreversible chemical fixation:

  - inefficient in immobilizing membranes,
  - can lead to protein extraction,
  - can cause artifical clustering.

Proposed solution: reversibly arrest (***cyro-arrest***) the cells at -45°C in medium containing dimethyl-sulfoxide (DMSO) to prevent formation of ice crystals.

Development

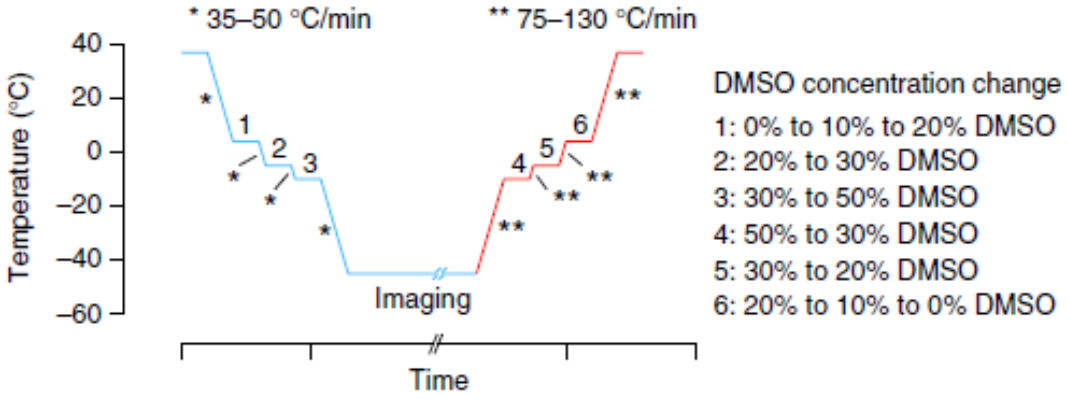

DMSO concentration change
1: 0% to 10% to 20% DMSO
2: 20% to 30% DMSO
3: 30% to 50% DMSO
4: 50% to 30% DMSO
5: 30% to 20% DMSO
6: 20% to 10% to 0% DMSO

Binary phase diagram

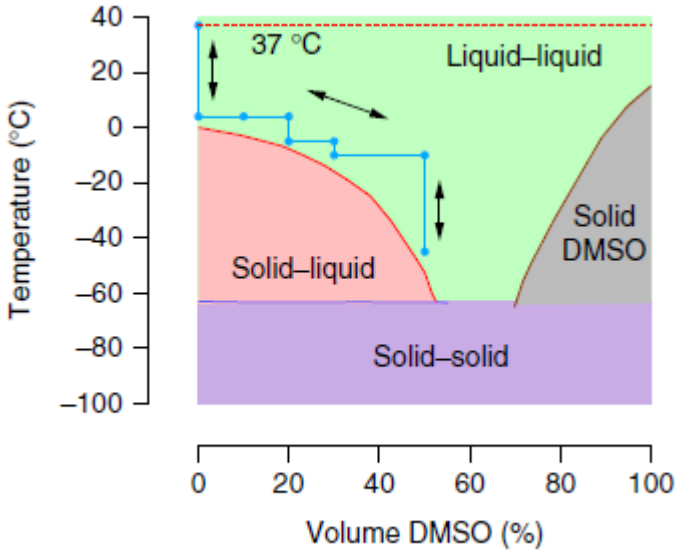

Time course:

1. Cells cooled to 4°C and medium replaced with HEPES-buffered medium containing 20% DMSO in 2 incremental steps of 10%.
2. Temperature decreased stepwise while the concentration of DMSO was increased to stay above the liquidus temperature.

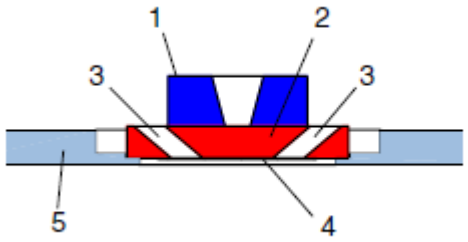

Cryo-stage:

1. Silver block
2. Aluminium block
3. Medium inlet and outlet
4. 100 µm thick channel for the sample
5. Insulating PVC plate

Validation

- Efficiency of protein immobilization:

  - FRAP of the transmembrane EGFR-mCirtine and cytosolic eGFP

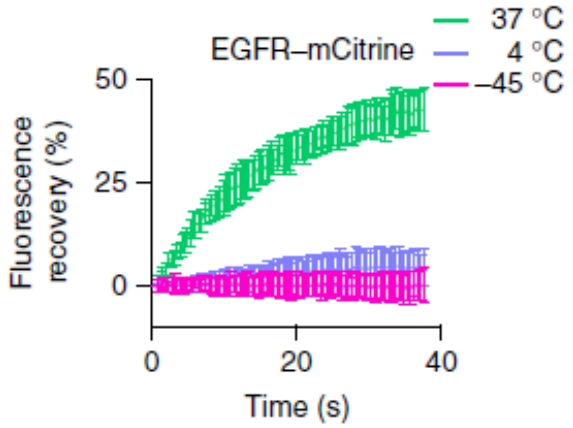

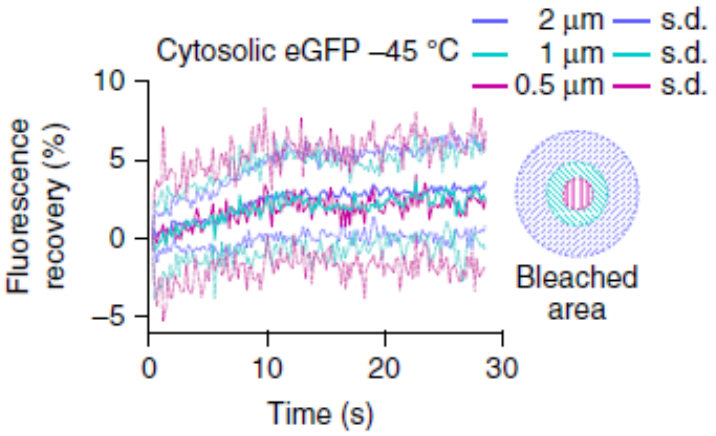

  - single-particle tracking of Cy3-labeled SNAP-EGFR in HeLa cells

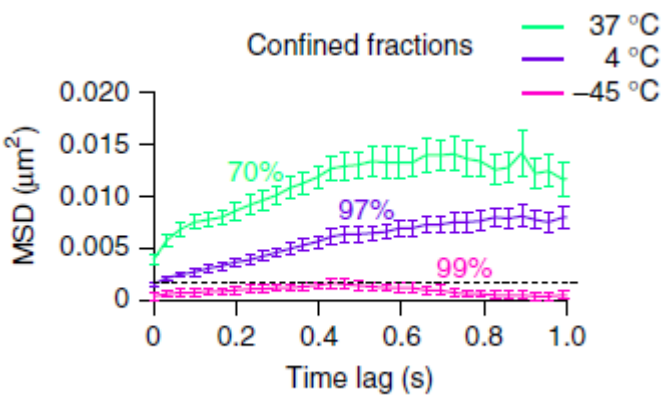

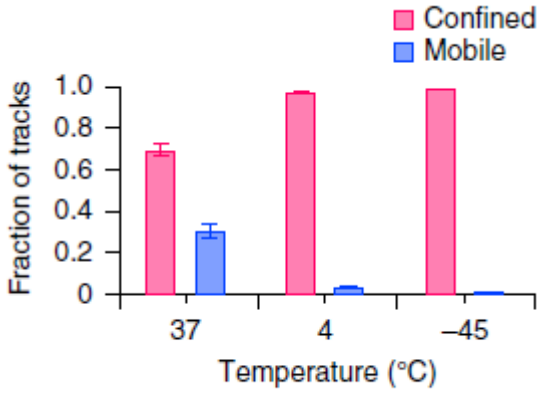

MSD=mean squared displacement

Reversibility I.

Survival of 5 different cell types, after 3 consecutive cryo-arrest cycles: PI staining and cytoplasmic eGFP to monitor cellular morphology.

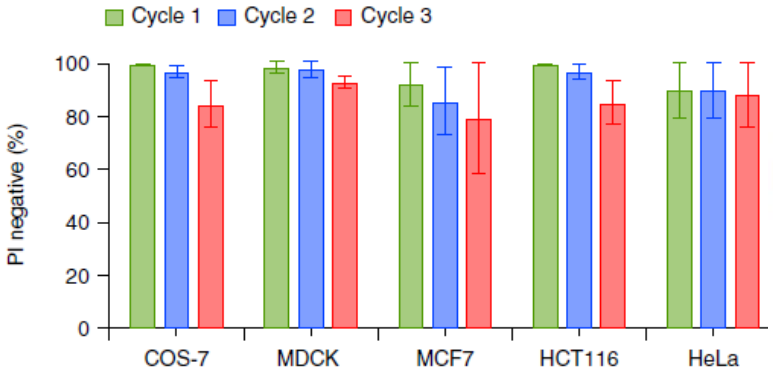

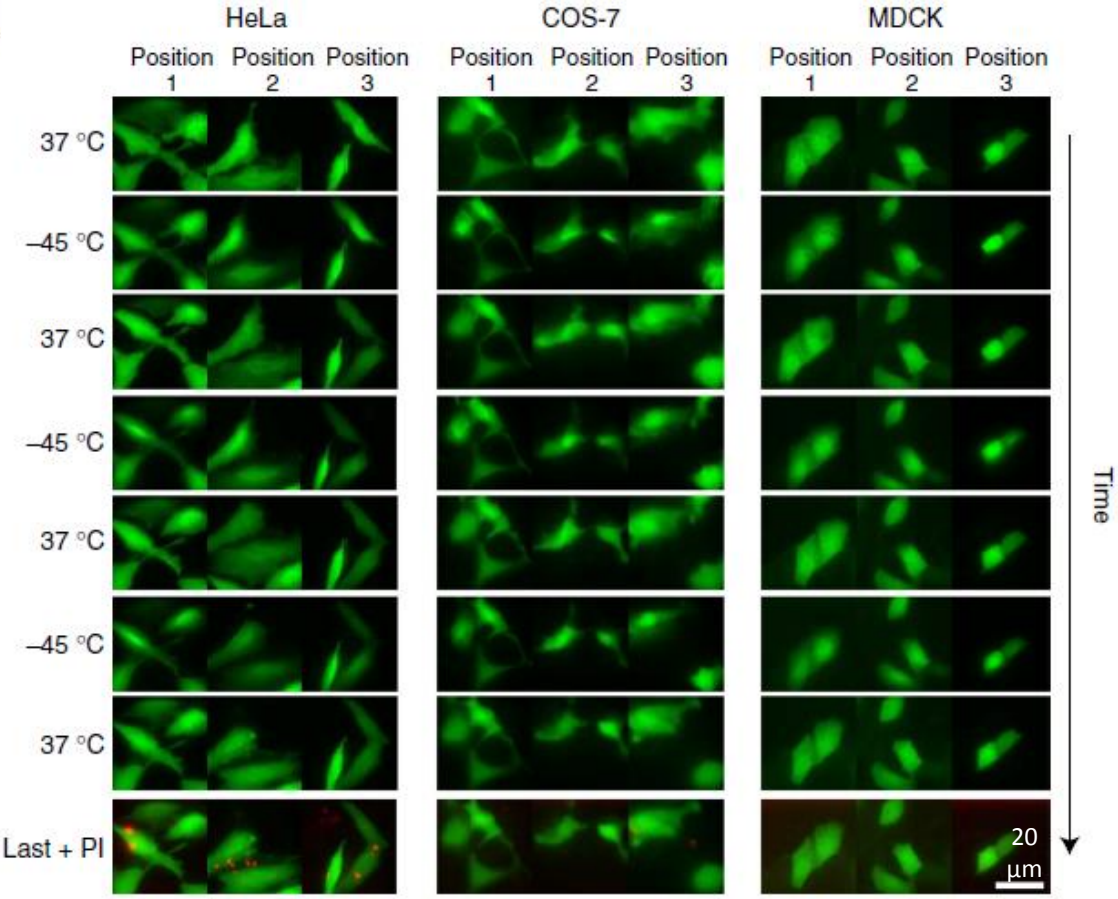

Reversibility II.

EGF signaling: 1. activity of EGFR measuring it with EGFR-mCitrine and phosphotyrosin-binding domain (PTB)-mCherry expressing HeLa cells.

FRET-FLIM time sequence

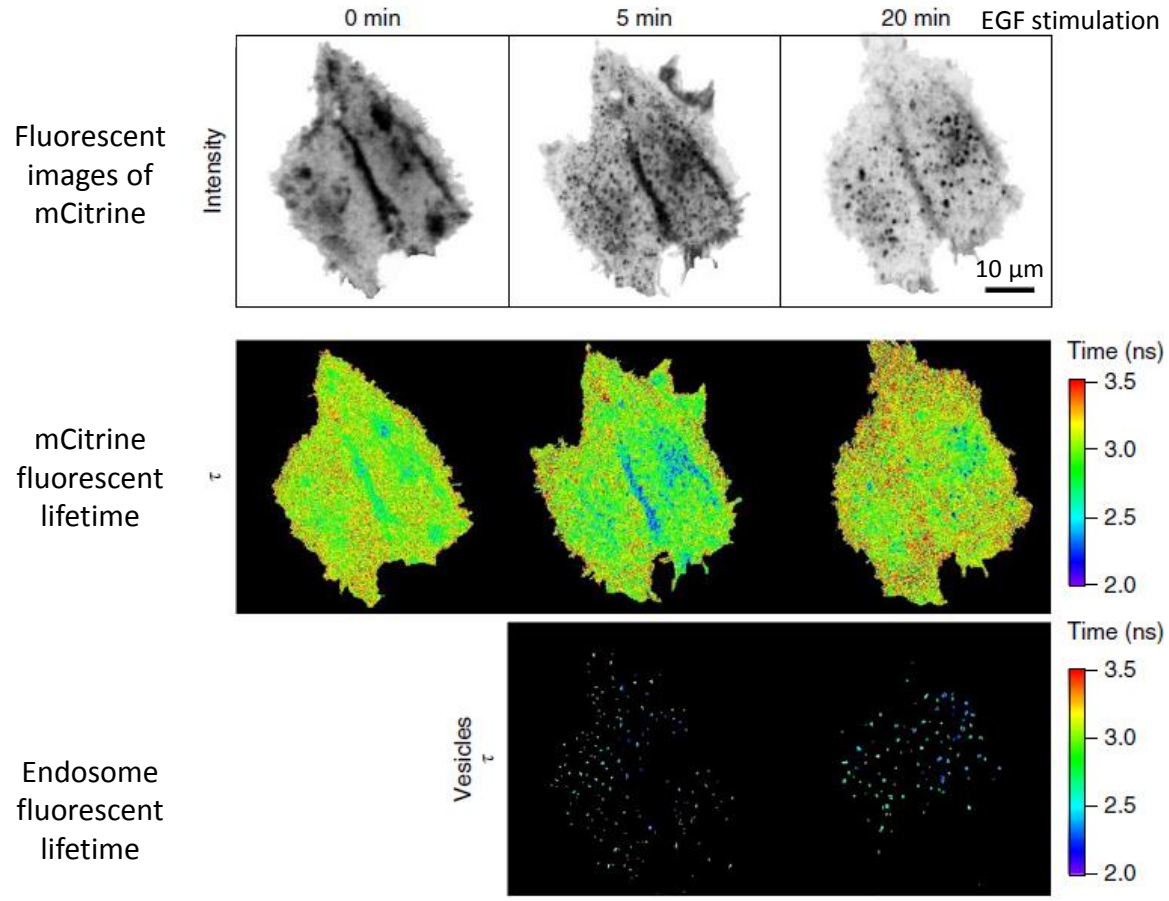

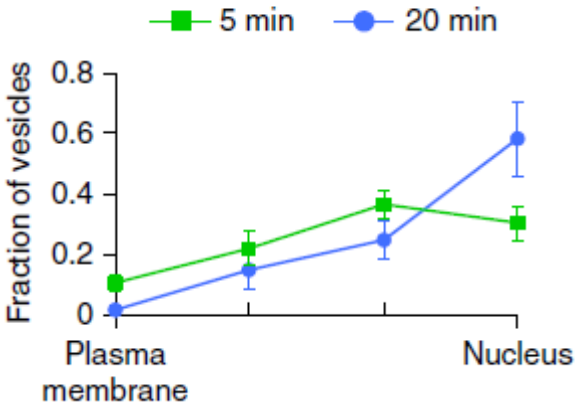

5 min of EGF stimulation after 1 cryo-cycle, that continued over 2 additional cyro-arrests at 5 and 20 mins.

Ligand-induced receptor endocytosis was fully functional after 3 cyro-arrest

Reversibility II.

EGF signaling: 2. activity of a downstream effector of EGFR, the extracellular signal-related kinase (ERK) in HeLa cells using a fluorescent kinase translocation reporter (KTR).

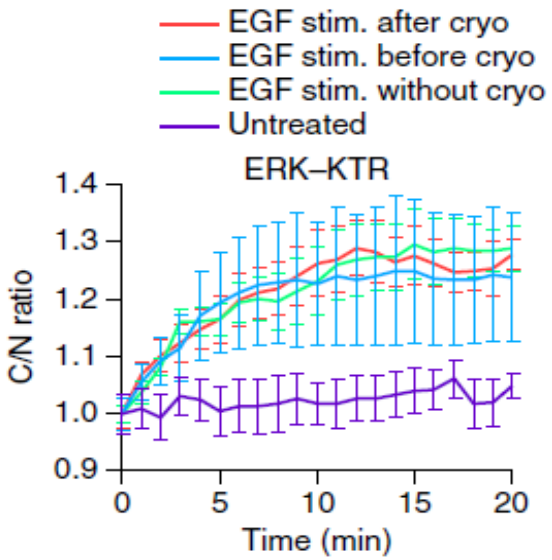

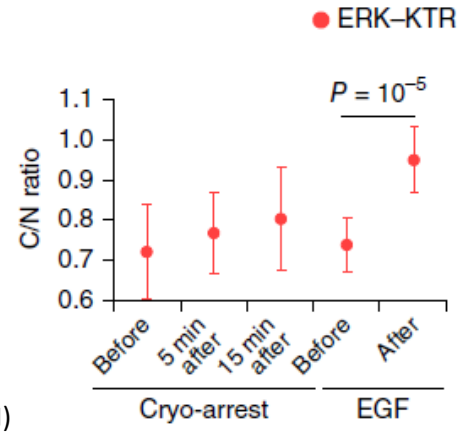

whole-cell over nuclear fluorescence intensity (C/N)

ERK activity:

1. upon EGF stimulation without cryo-arrest (EGF stim. without cryo),
2. upon 2 min EGF stimulation after cryo-arrest (EGF stim. after cryo),
3. upon cryo-arrest 2 min after EGF stimulation (EGF stim. before cryo)
4. and unstimulated cells (untreated).

No impairment of ERK response by cryo-arrest before or after EGF stimulation and cryo-arrest alone did not induce ERK response

Testing stress-response

Measured the activity of the stress-activated protein kinase JNK and the cold-activated protein kinase p38 MAPK31 using their respective KTRs.

Investigated the mRNA level of the heat shock protein HSP70 and the cold-stress protein CIRBP.

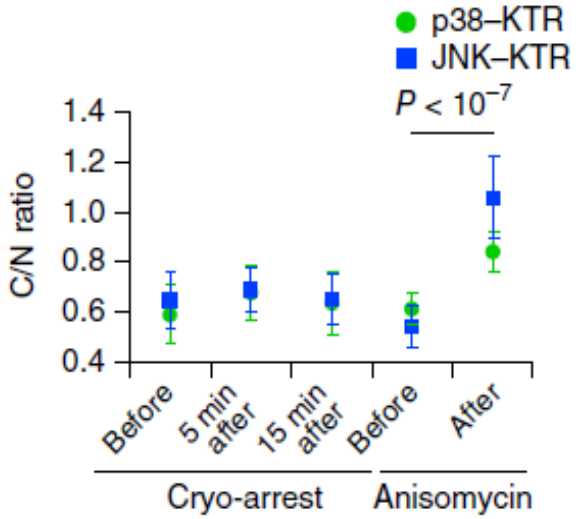

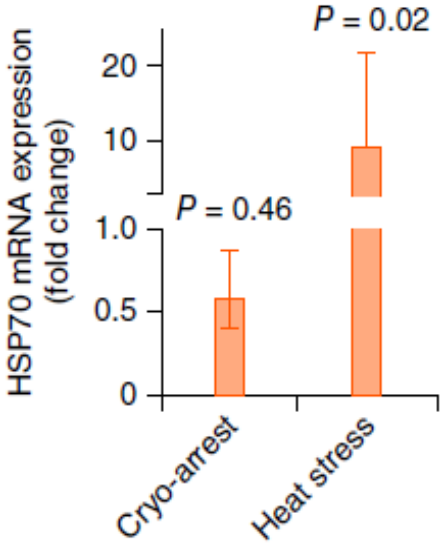

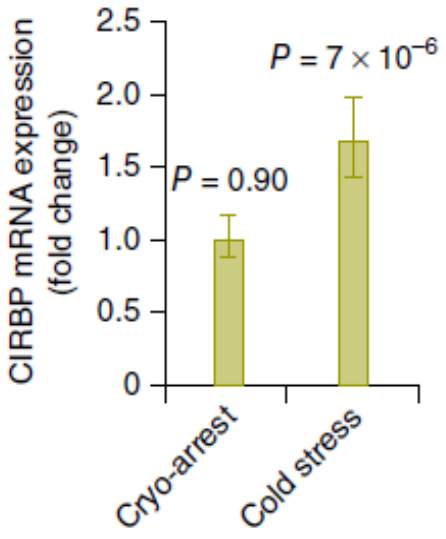

15 min after cryo-arrest;
Heat stress: 30 min at 42°C;
Cold stress: 24 hour at 32°C.

Nanoscale organization of EGFR during cryo-arrest

Cryo-arrested HeLa cells expressing EGFR–mEos2 before and 5 min after EGF stimulation.

Invesigated with TIRF-PALM.

Distance <40 nm, molecules in clusters (EGFR dimer~12 nm).

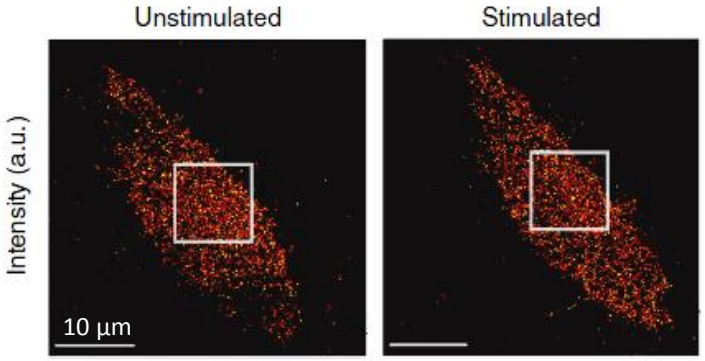

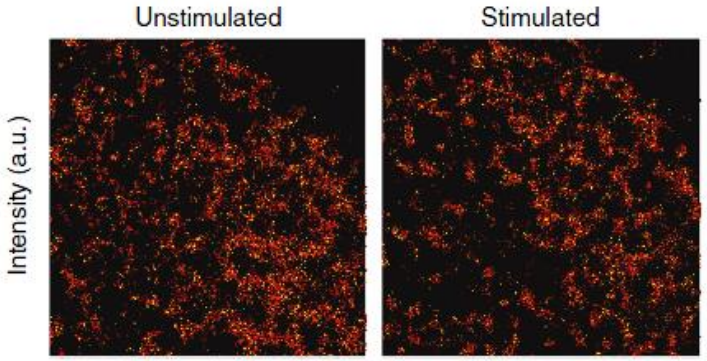

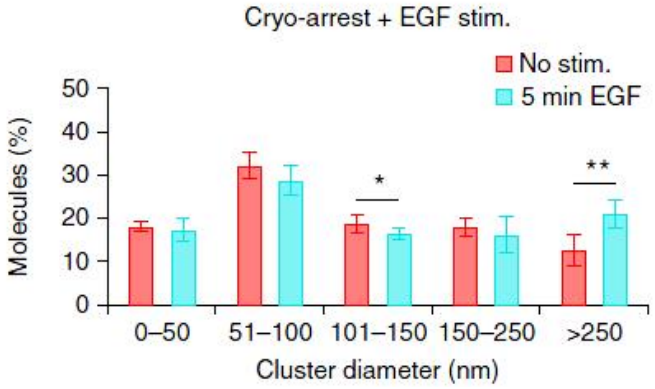

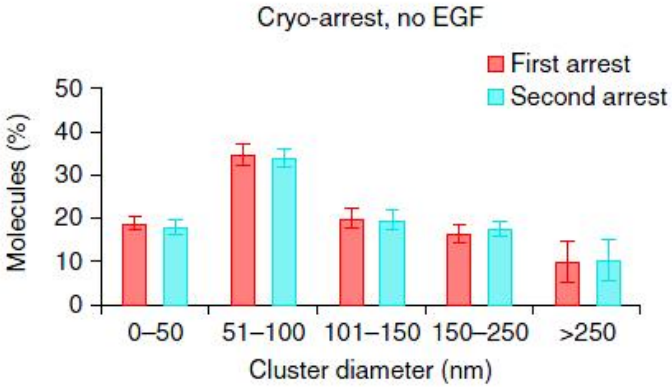

Receptors in clusters d=10s to 100s of nm before; d=250 nm after EGF stimulation.

Consecutive cryo-arrests without stimulation did not show any differences in clustering parameters.

Nanoscale organization of EGFR during cryo-arrest

To assess self-association: homo-FRET between mCitrines inserted into EGFR via a linker (EGFR–QG–mCitrine) by fluorescence anisotropy.

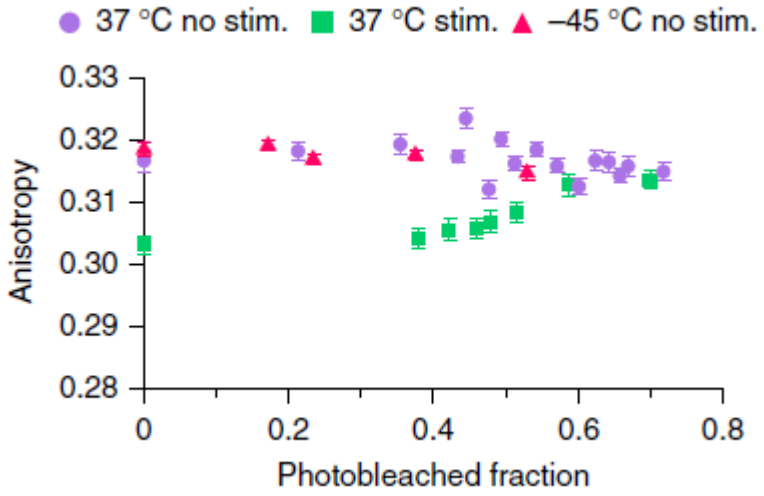

EGFR–QG–mCitrine showed no significant increase in anisotropy

indicating that EGFR before stimulation is mainly monomeric, therefore the cluster was not due to self-association

Microscale organization of EphA2 during cryo-arrest

- spatial distribution of the active conformation of EphA2
- before and after stimulation with clustered ephrin A1 fused to Fc region of human IgG1 antibody (ephrinA1–Fc)
- in COS-7 cells expressing LIFEA2

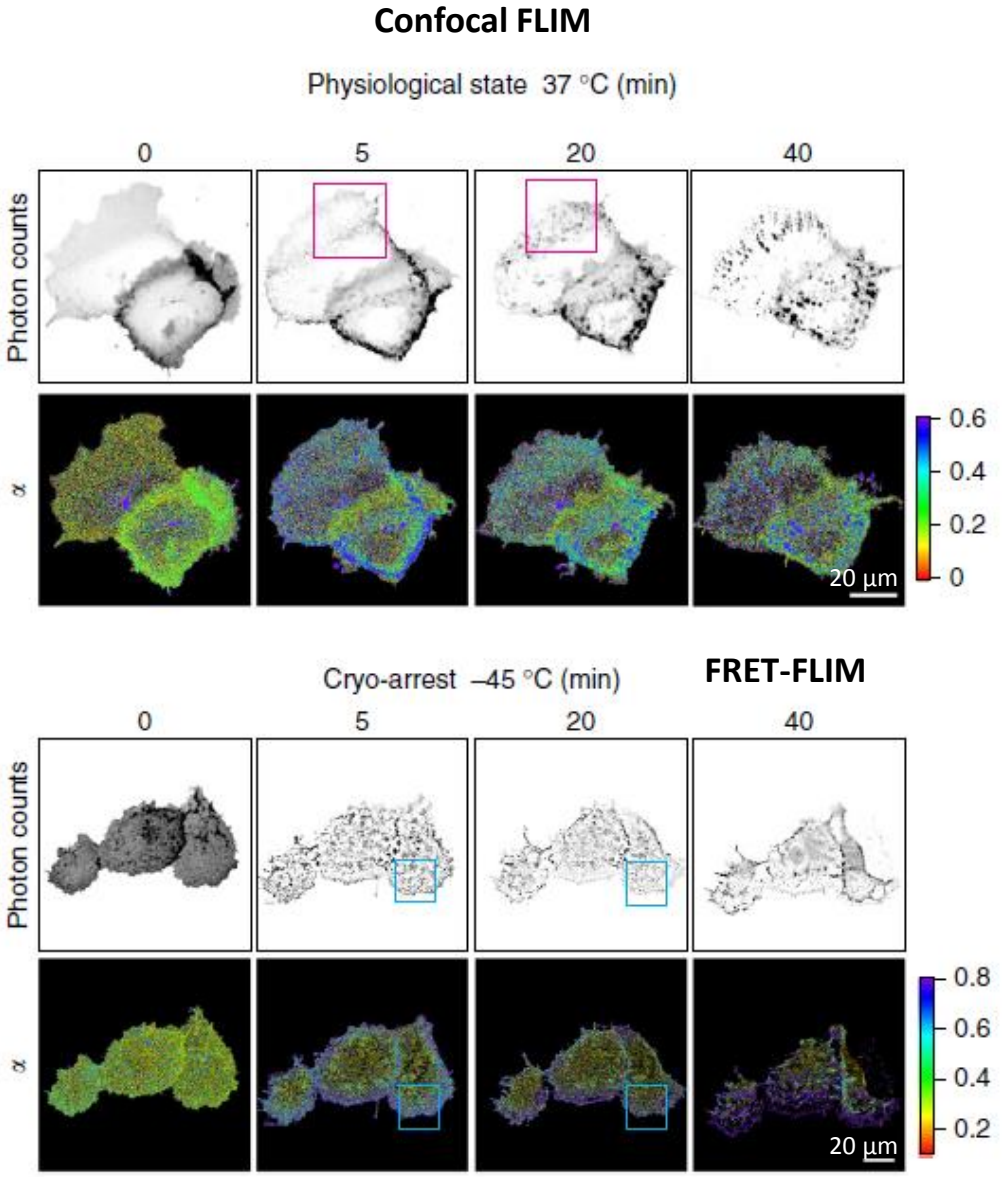

Microscale organization of EphA2 during cryo-arrest

- spatial distribution of the active conformation of EphA2
- before and after stimulation with clustered ephrin A1 fused to Fc region of human IgG1 antibody (ephrinA1–Fc)
- in COS-7 cells expressing LIFEA2

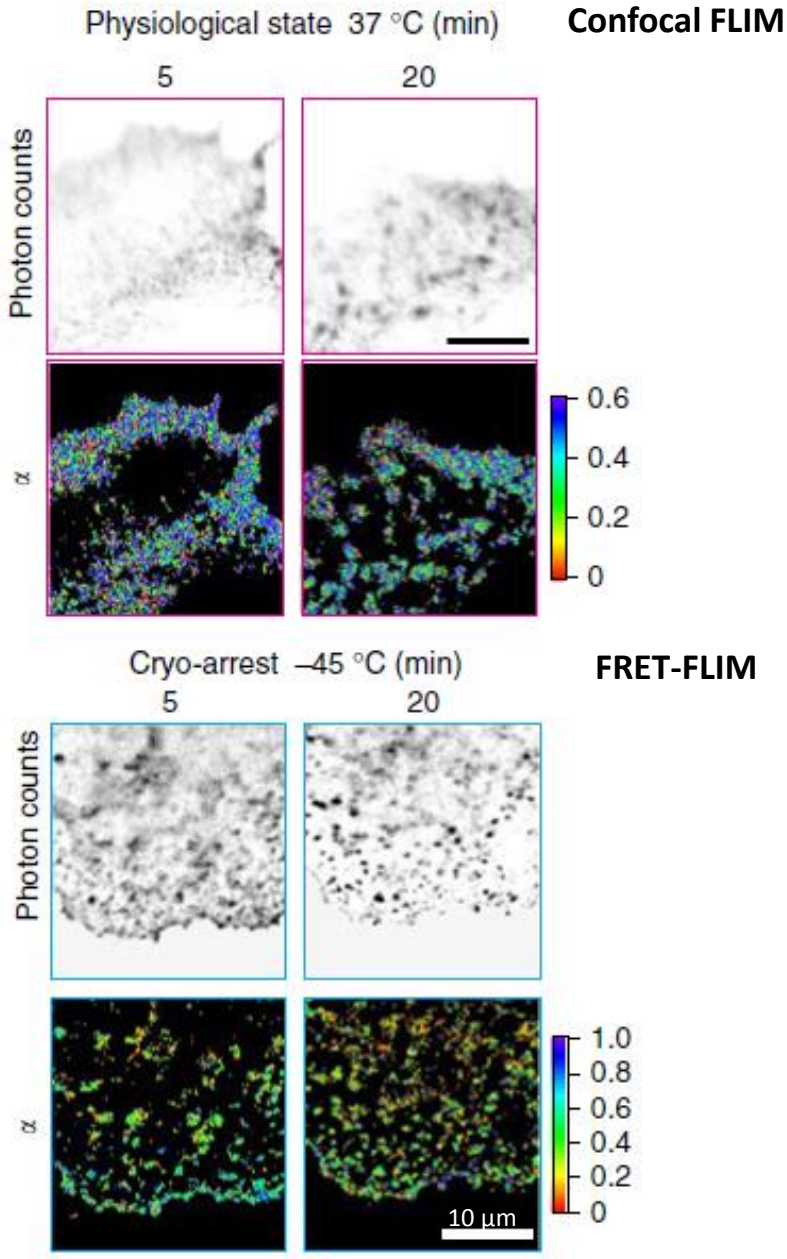

LIFEA2 in its active state resides at the plasma membrane.
20 and 40 min after stimulation, blurred structures appeared in the cytoplasm.

Conclusion

- Improvements:

  - enables physical fixation: imaging with long exposure times of arrested, but living, cells;

  - compatible with the use of immersion objectives;

  - DMSO ensures cryo-tolerance without cytotoxicity at low temperatures without disrupting molecular interactions;

  - the conditions used were able to stop residual diffusion of the molecules.

- Limitations:

  - has to be verified in each case.

nature COMMUNICATIONS

ARTICLE

Received 22 Mar 2016 | Accepted 5 Jul 2016 | Published 12 Aug 2016

DOI: 10.1038/ncomms12471 OPEN

Fast live-cell conventional fluorophore nanoscopy with ImageJ through super-resolution radial fluctuations

Nils Gustafsson[1,2,*], Siân Culley[1,*], George Ashdown[3], Dylan M. Owen[3], Pedro Matos Pereira[1] & Ricardo Henriques[1]

Rationale

PALM and STORM: for structural cellular biology.

SIM: suitable for live cell imaging, but requires expensive optical equipment.

Live cell SMLM depends on the capacity to detect enough fluorophores to super-resolve structures, in a time small enough to minimize motion-blur artefact.

Algorithms: >1,5 µm, but high density samples are still challenging (deconSTORM, 3B and SOFI).

- *Proposed solution:* **super-resolution radial fluctuations (SRRF)**, analysis of a sequence of images acquired in a standard widefield or total internal reflection fluorescence (TIRF) microscope directly generates a superresolution reconstruction without fluorophore detection and localization.

NanoJ SRRF software package

- SRRF calculates the degree of local gradient convergence (referred to here as ***radiality***) across the entire frame, on a sub-pixel basis. – Information in the gradient field is preserved for ***further temporal analysis***.
- This radiality distribution is capable of distinguishing two Gaussian PSFs separated by 1.7 times the PSF.
- The distribution is independent of PSF intensity and changes in PSF size and preserves deformations of the PSF.
- Non-fluorophore-associated radiality peaks - uncorrelated in time.

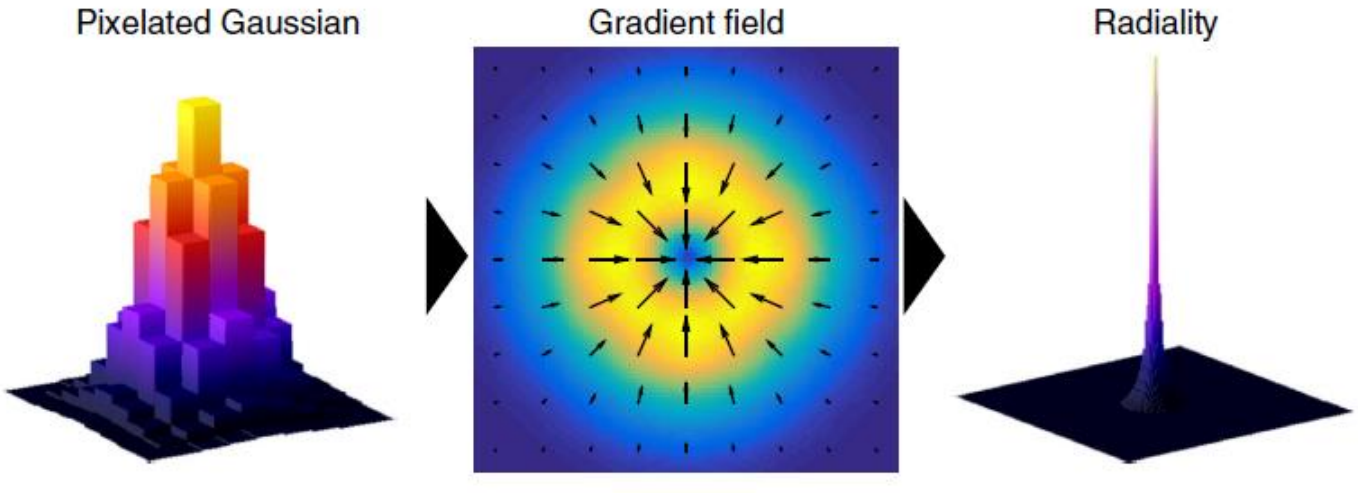

In silico characterization

- Simulated data with varying fluorophore kinetics, resulting in different fluorophore densities.
- At low densities: limited precison was obtained, greater separation was obtained for constantly emitting fluorophores, exhibiting an intensity fluctuation.

Fluorophores placed every 5 nm along the line

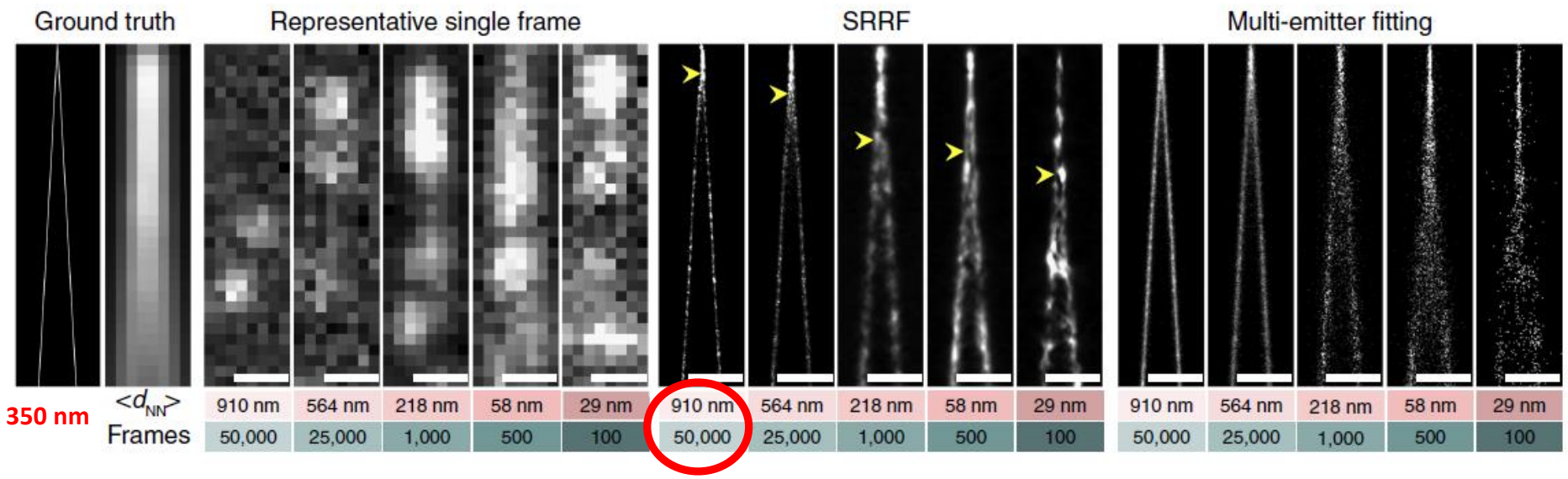

mean emitting fluorophore separation, d_{NN}

Failed to reconstruct the structure at these ultra-high-fluorophore densities

In silico characterization

- Fixed microtubules labelled with Alexa Fluor 647.
- 2 microtubules separated by ~75nm can be resolved at low densities.
- Enables the use of **fast**, **low illumination intensity** imaging regimes compatible with **conventional fluorophores** in living cells.

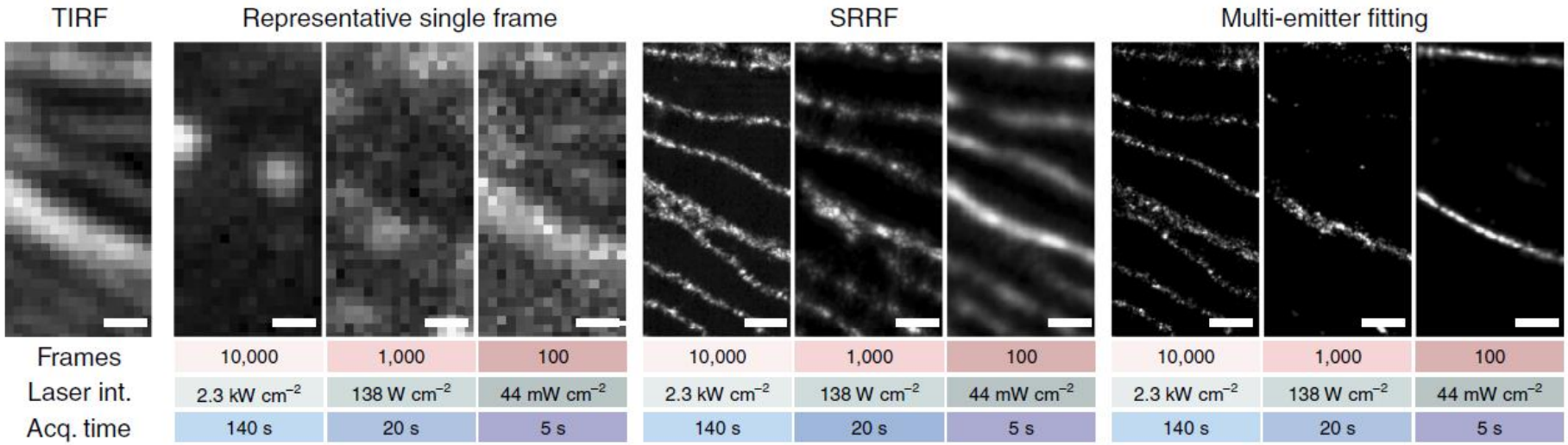

Applicability to different imaging modalities

Alexa Fluor 647 labelled microtubules:

1. high-intensity laser-illuminated widefield epifluorescence, generating a low-density STORM-like data set
2. low-intensity LED-illuminated widefield epifluorescence, generating an high-density data set
3. Laser scanning confocal, generating an ultra-high-density data set

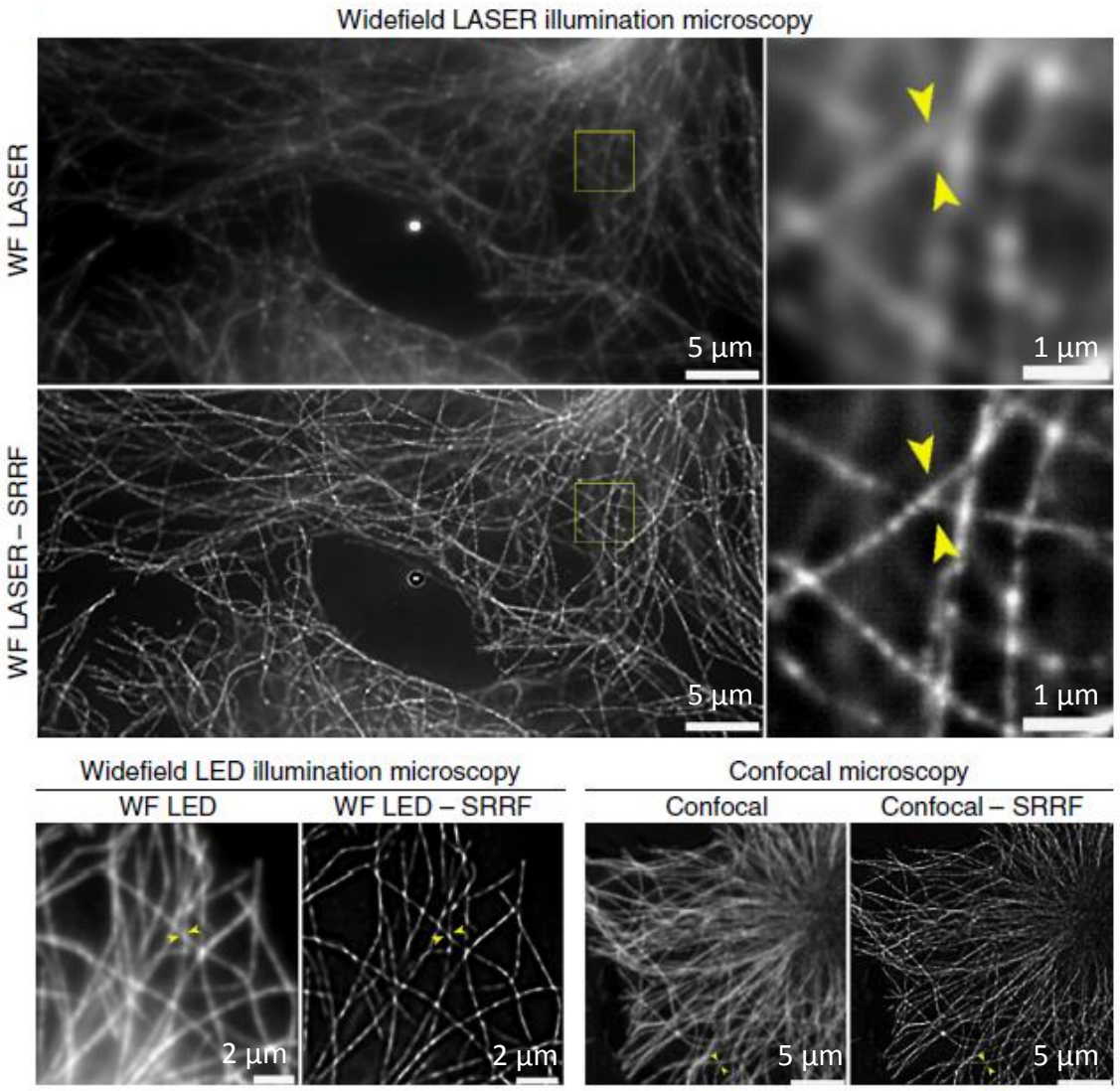

Applicability to different imaging modalities

Achievable resolution:

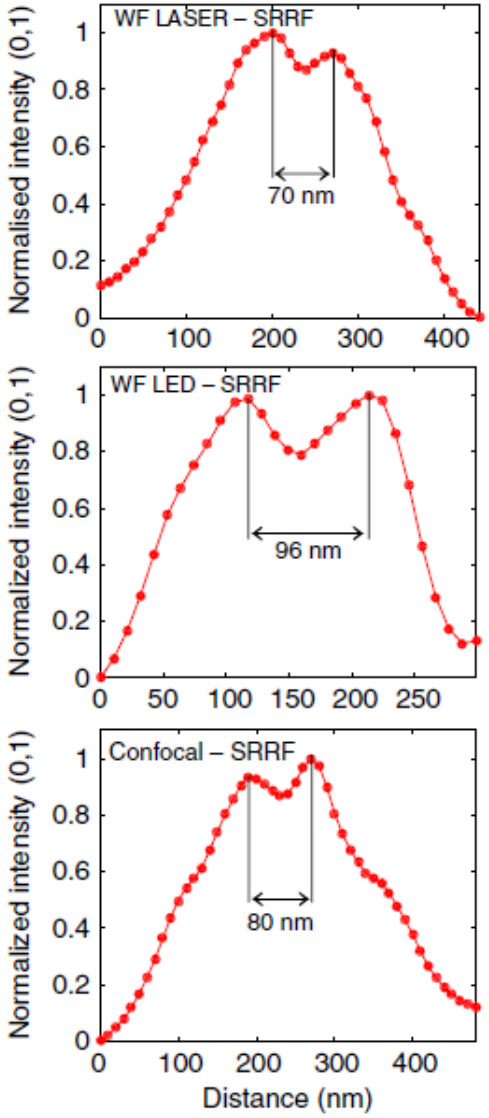

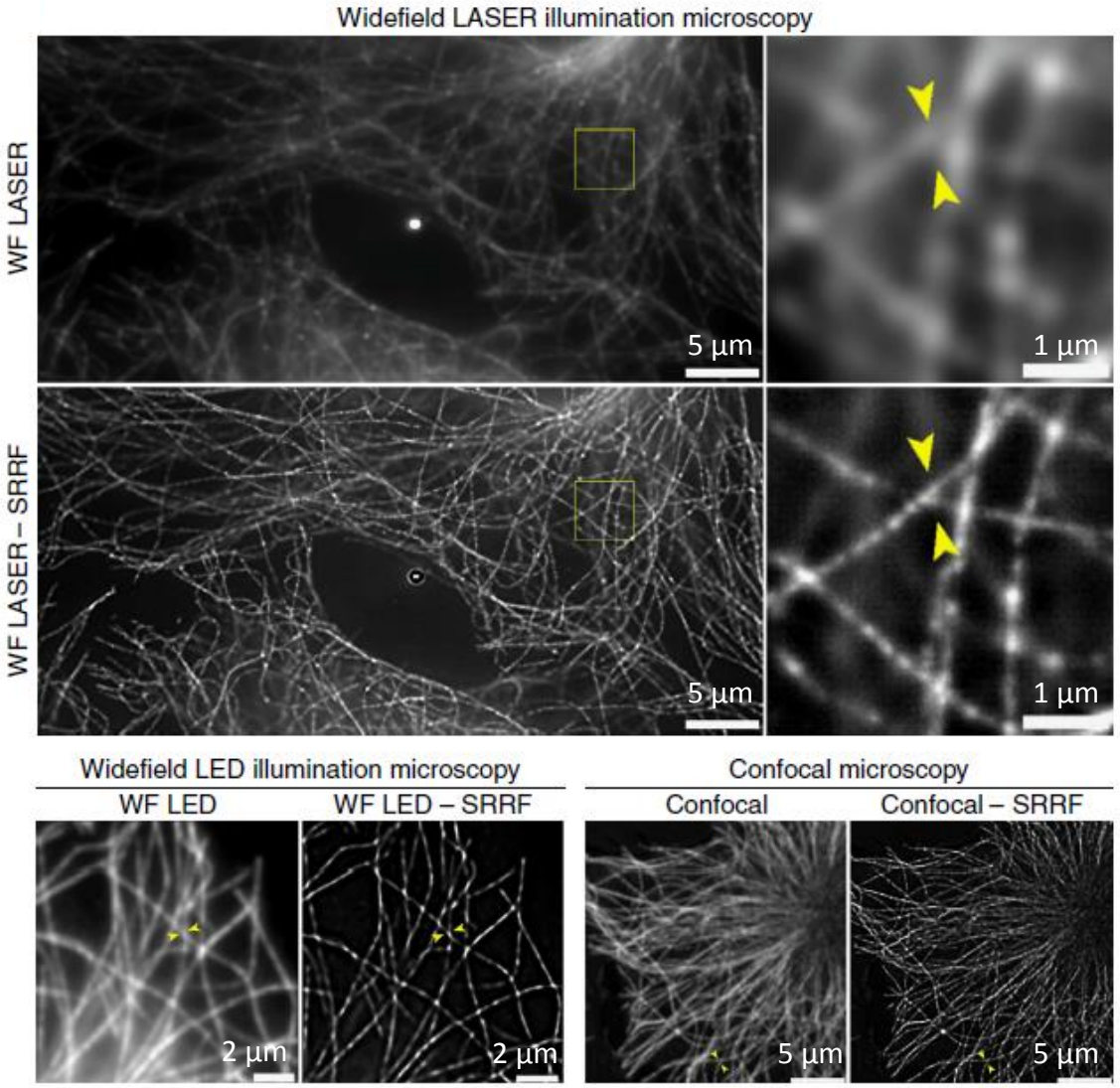

Imaging actin cortex dynamics in the immunological synapse

Jurkat T cells transfected with LifeAct-GFP dropped onto a coverslip coated with antibodies to emulate the formation of a synapse after T-cell receptor engagement.

The density of the actin varies significantly across the synapse.

Particle image velocimetry (PIV): directionality and relative speed encoded in different colours.

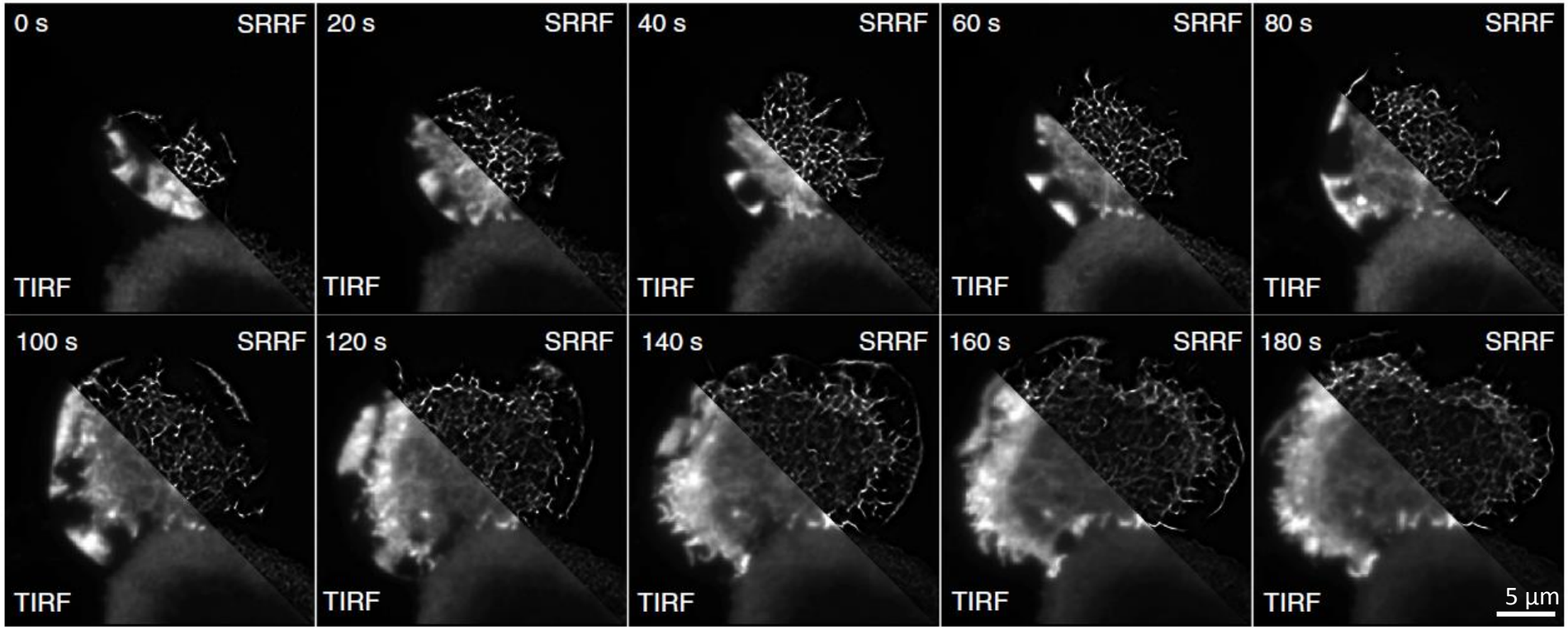

Imaging actin cortex dynamics in the immunological synapse

Jurkat T cells transfected with LifeAct-GFP dropped onto a coverslip coated with antibodies to emulate the formation of a synapse after T-cell receptor engagement.

The density of the actin varies significantly across the synapse.

Particle image velocimetry (PIV): directionality and relative speed encoded in different colours.

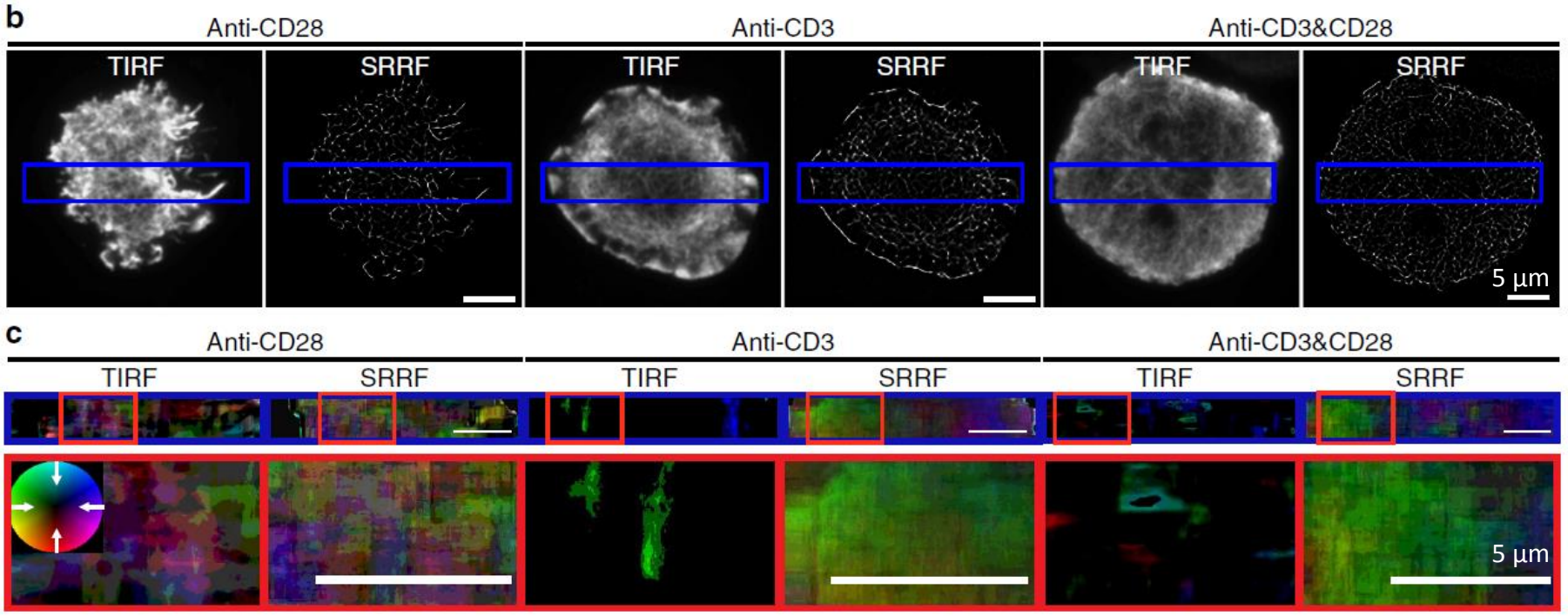

Central colour (minimum intensity): 0 µm/min,
saturated colours (maximum intensity): 38.4 µm/min.

Retrograd flow

Conclusion

- Improvements:

  - technique for both fixed-cell and dynamic live cell superresolution using conventional fluorophores;

  - compatible with different imaging modalities;

  - significant reduction in reconstruction artefacts

- Limitations:

  - was not compared to SIM;

  - has to be verified in each case.

Thank you for your attention!

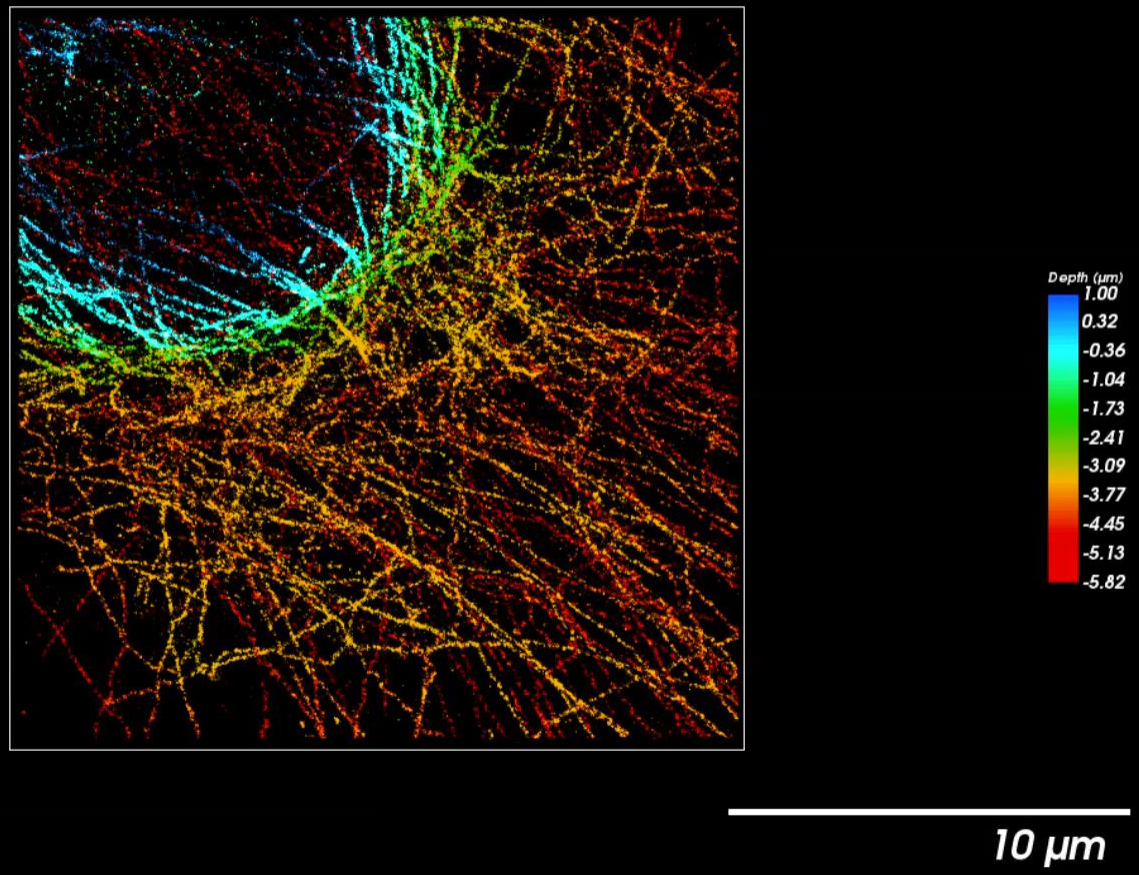

Microtubules in HeLa cells

Image: Microscopy Winter School, UZH, 2017.